



## Thermal Radiation and Viscous Dissipation Effects on (MHD) Bioconvection Stream of Maxwell Nanoliquid over a Permeable Vertical Plate Due to Gyrotactic Microorganisms

Thummala Sankar Reddy<sup>1</sup>, Parakapali Roja<sup>2</sup>, Shaik Mohammed Ibrahim<sup>3</sup>, Giulio Lorenzini<sup>4\*</sup>

<sup>1</sup> Department of Mathematics, Annamacharya Institute of Technology and sciences, C. K. Dinne, Kadapa 516003, A.P., India

<sup>2</sup> Department of Mathematics, Annamacharya Institute of Technology and sciences, Rajmpeta, Kadapa 516126, A.P., India

<sup>3</sup> Department of Mathematics, Koneru Lakshmaiah Education Foundation, Vaddeswaram, Guntur, A.P. 522302, India

<sup>4</sup> Department of Engineering and Architecture, University of Parma, Parco Area delle Scienze 181/A, Parma 43124, Italy

Corresponding Author Email: [giulio.lorenzini@unipr.it](mailto:giulio.lorenzini@unipr.it)

<https://doi.org/10.18280/mmep.090205>

### ABSTRACT

**Received:** 22 March 2022

**Accepted:** 13 April 2022

#### Keywords:

*thermal radiation, viscous dissipation, MHD, bioconvection, Maxwell nanoliquid, microorganisms*

This manuscript deliberates on thermal radiation and viscous dissipation possessions on magneto-hydrodynamic (MHD) bioconvection stream of a new variety of water established the upper-convected Maxwell, Nanoliquid covering Nanoparticles and motile gyrotactic microorganisms over an absorptive vertical moving plate. Nanoliquid bio convective is developed through the mutual possessions of buoyant forces and magnetic field on the collaboration of motile microorganisms and Nanoparticles. The leading nonlinear PDE of the problem are transforming into a structure of nonlinear ODE over suitable similarity conversion and shooting method procedure joined with Runge–Kutta–Fehlberg integration pattern, the exemplary BVP is attempted numerically. A parametric investigation of the complete stream regime is supported out to demonstrate the possessions of the leading constraints, specifically bioconvection Lewis quantity  $Lb$ , traditional Lewis quantity  $Le$ , bioconvection Peclet quantity  $Pe$ , buoyancy quotient constraint  $Nr$ , bioconvection Rayleigh quantity  $Rb$ , Brownian motion constraint  $Nb$ , thermophoresis constraint  $Nt$ , Hartmann quantity  $Ha$ , Grashof quantity  $Gr$ , radiation constraint  $R$  Eckert quantity  $Ec$ , microorganisms concentration variance constraint  $\Omega$  and a suction/injection constraint  $fw$  on the flow, temperature, volume fraction of nanoparticles and motile microorganisms density outlines as well as the friction quantity, the local Nusselt quantity, the local Sherwood quantity and the local density quantity of the motile microorganisms.

## 1. INTRODUCTION

Bioconvection flow is used to pronounce the occurrence of macroscopic convective motion of the liquid initiated due to the gradient of density generated by united spinning of microorganisms. These self-propelled motile microorganisms inclines to concentrate close the upper portion of the liquid sheet, and this accumulation makes the upper sheet much thicker than the lower section and eventually yield variability, which consequences in producing the several movement outlines into the scheme [1-6]. Bioconvection has abundant applications in biological and bio-microsystems, for case, enzyme biosensors and biotechnology due to the momentum transport improvement and collaborating, which are significant concerns in many micro-systems. Microbial-enhanced oil reposition is another potential use of bioconvection theory, in which microorganisms and nutrients are inoculated in oil-bearing stratum to correct permeability variation. In a broader sense, the ability of motile microorganisms to spin in a specific way can be utilised to extract information from cells, purify principles, and distinguish between various sub-populations (for example, to distinguish fast swimmers from sluggish [7-9]). In these presentations, bioconvection would avoid effective separation as it would basis collaborating among dissimilar kinds of cells.

Bioconvection schemes, on the other hand, can be classified based on the directional movement of various types of microorganisms, but they all spin in an upward direction (having larger density than the base liquid). For example, chemotaxis or oxytactic microorganisms spin upward due to a gradient in oxygen concentration because they require a specific amount of oxygen to be active, gyrotactic microorganisms whose swimming direction is determined by a balance in viscous and gravitational torques, and geotactic microorganisms spin alongside gravitational possessions [10, 11]. In accumulation, the model of nanoliquid bioconvection has also comprehensive circle of applications, for example, nanomaterial dispensation, automotive coolants, purification process of medical suspensions, polymer covering and intellectual structure plan. The idea of nanoliquid bioconvection was principal presented by Kuznetsov [12-14] and later on numerous authors and analysts explored the communication of nanoliquid with bioconvection underneath numerous physical circumstances [15-20].

The Maxwell liquid belongs to the sub class of rate type of liquids. This liquid model predicts the relaxation time belongings. Liquids belong to the differential type cannot predict such effects. Stability scrutiny method of Maxwell liquid in porous medium past an elongating sheet was addressed by Wang and Tan [21]. Nadeem et al. [22]

considered the numerical behaviour for Maxwell liquid past an elongating surface in accordance with nanoparticles. Ramzan et al. [23] presented optimal solution for Maxwell stream at nanostructure level. Nagendramma et al. [24] scrutinized the multiple slips and radiation belongings of Maxwell nanoliquid stream phenomenon. Hayat et al. [25] demonstrates Maxwell nanoliquid stream in 3D platform. The upper convected Maxwell liquid (UCM) is one of the visco-elastic liquids. Sakiadis steady stream of UCM over a stiff external was communicated by Sadeghy et al. [26]. Succeeding Taylor series linearization approach for UCM approved by porous elongating surface was exemplified by Motsa et al. [27]. Coupled heat and momentum consequence of UCM liquid over a stirring surface was analyzed by Hayat et al. [28]. Heat transport interrelated study of UCM liquid was described by Vajravelu et al. [29].

The way disciplines of fish and flocks of birds benefit from the presence of others can be learned from nature. Fish and birds fundamentally position themselves in hydrodynamically effective configurations when migrating in flocks. Microorganisms can also change their surroundings in large numbers, whether intentionally or unintentionally, using a mechanism known as bioconvection. The spinning of microorganisms commonly causes the nearby liquid to be prolonged, causing the liquid to convect. Furthermore, the resulting large-scale liquid flow improves mixing and nutrient source. Kuznetsov [30-32] was the first to recognize bioconvection as the movement or upswing of motile microbe suspensions. Geng and Kuznetsov investigated the interaction between bacteria and nanoparticles [33-35].

It is clear that immovability of nanoparticles develops over the addition of gyrotactic microorganisms. The influence of gyrotactic microbes for occasion algae and bacteria in stream of nanoliquids due to elongating/shrinking sheet is examined by Zaimi et al. [36]. Tham et al. [37] scrutinized the sundry convection stream of nanoliquid containing gyrotactic microorganisms towards a solid sphere surrounded in a porous medium. Aziz et al. [20] addressed the free convection border stratum stream of nanoliquid covering motile microorganisms. Xu and Pop [38] explored the completely established sundry bio-convection stream of nanoliquid occupied in a flat channel embracing the nanoparticles and gyrotactic microorganisms. Khan et al. [39] investigated the properties of nanoparticles and gyrotactic microorganisms in a non-Newtonian liquid free convection stream enclosed by a porous material. According to Ibrahim and Makinde [40], it plays an important function in monitoring the concentration and temperature differences between hydrogen and oxygen in the environment, which may influence the rate at which different types progress. Alsaedi et al. [41] and Ramzan et al. [42] investigate the effects of magneto-hydrodynamics (MHD) and asymmetrical convection in a stretchable stream of viscous nanomaterial with gyrotactic microorganisms. Liquid stratification is unquestionably caused by changes in concentration and temperature, as well as the mixing of liquids with different densities. When both heat and momentum transfers are current at the same time, it's intriguing to investigate the influence of double stratification.

Furthermore, the study of streams in the presence of double stratification and sundry convection has numerous applications in the field of manufacturing, including heat dissipation into the atmosphere through seas, lakes, and rivers, thermal energy storage through solar ponds, and heat transport from thermal sources through power plant condensers. There

have been some attempts to investigate the impression of double stratification with sundry convection. For example, Srinivasacharya and Surender [43] discovered double stratification properties in a nanoliquid stream with various convection. Hayat et al. [44, 45] describe the appearance of twofold stratification over an elongating sheet and cylinder in the presence of thermal radiation and sundry convection. Hayat et al. [46] recently looked at the perception of double stratification in stream of viscous liquid with sundry convection.

In the vast majority of industrial and physiological transactions, the repute of non-Newtonian liquids appears to be rather evident. Disparity, main, and rate kinds are the most used classifications for these liquids. The considered model belongs to the rate category resource grouping and has the capacity to designate relaxation time features. In the extrusion of a polymer expanse from a die or the drawing of malleable films, a rate type model is applied. Because of its simplicity, the Maxwell classical theory has gained a lot of attention from recent researchers.

The rigorous solution for helical streams of Maxwell liquid with shear stress on the border was investigated by Jamil and Fetecau [47]. Zierp and Fatecau [48] investigate the Rayleigh-Stokes problem using Maxwell liquid. Hayat et al. [49] investigate the effects of thermophoresis and Joule heating in an elongated stream of Maxwell liquid over a convective border condition. The heat transfer in a Maxwell liquid subjected to thermal radiation and viscous dissipation above an extended surface was obtained by Hsiao [50]. Ramzan et al. [51] presented optimal solutions for various convective Maxwell nanomaterials.

According to the findings, the effects of thermal radiation and viscous dissipation on the bioconvection MHD stream of Maxwell nanoliquid including nanoparticles and gyrotactic microorganisms have yet to be investigated. Much for non-Newtonian liquids, the difficulty narrows even further. As a result, our primary aim is to look at the Maxwell nanoliquid stream that is constrained by a stretchable surface. Explicitly, the novelty of the existing examination is demonstrated by the following features. We must first investigate the impact of gyrotactic bacteria. Furthermore, the analysis should be carried out in the context of Magneto-hydrodynamics (MHD). After that, look into the thermal, solutal, and motile density stratifications. The effects of a variety of appropriate limitations on the flow, temperature, concentration, and motile density microorganism fields are investigated. The density of Nusselt, Sherwood, and motile is calculated.

## 2. MATHEMATICAL MODEL FORMULATION

We deliberate a stable border sheet flow of a water-based electrically conducting the upper convected Maxwell nanoliquid comprising gyrotactic microorganisms past a permeable vertical flat plate with thermal radiation. The stream is subjected to a uniform transverse magnetic field of strength  $B_0$ . There is no applied voltage and the magnetic Reynolds magnitude is small, hence the induced magnetic field and Hall effects are insignificant. As earlier mentioned, the occurrence of nanoparticles is supposed to have no result on the direction of microorganisms' swimming and on their spinning flow. It is supposed that the nanoparticle suspension is constant (there is no nanoparticle accumulation) and dilute (the concentration of nanoparticles is than 1%). This is a

logical notion, since nanoliquid bio-convection is predictable to occur only in a dilute suspension of nanoparticles; else, a large concentration of nanoparticles would consequence in increased viscosity of the base liquid, which would suppress bioconvection [14]. Adopting the Boussinesq estimate, at the same time, seeing thermophoresis and Brownian motion belongings due to nanoparticles according to the scheme developed by Buongiorno [15], while the model for bioconvection due to oxytactic microorganisms is based on the approach presented in Refs. [23, 24], the boundary-layer estimates of the continuity, momentum, energy, nanoparticle concentration and conservation for microorganisms equations are:

(i) Continuity:

$$\frac{\partial u}{\partial x} + \frac{\partial v}{\partial y} = 0 \quad (1)$$

(ii) Momentum:

$$\begin{aligned} u \frac{\partial u}{\partial x} + v \frac{\partial u}{\partial y} = & -\frac{1}{\rho_f} \frac{\partial p}{\partial y} + v_f \frac{\partial^2 u}{\partial y^2} + k_1 \frac{\partial N}{\partial y} - \frac{\sigma B_0^2 u}{\rho_f} \\ & + k_0 \left[ u^2 \frac{\partial^2 u}{\partial x^2} + v^2 \frac{\partial^2 u}{\partial y^2} + 2uv \frac{\partial^2 u}{\partial x \partial y} \right] \\ & + \frac{1}{\rho_f} \left[ (1 - \phi_\infty) \rho_f \beta g (T - T_\infty) - (\rho_p - \rho_f) g (\phi - \phi_\infty) \right. \\ & \left. - (\rho_m - \rho_f) g \gamma (n - n_\infty) \right] \end{aligned} \quad (2)$$

(iii) Equation of energy:

$$\begin{aligned} u \frac{\partial T}{\partial x} + v \frac{\partial T}{\partial y} = & \alpha \left( \frac{\partial^2 T}{\partial x^2} + \frac{\partial^2 T}{\partial y^2} \right) - \frac{1}{\rho c_p} \frac{\partial q_r}{\partial x} \\ & + \tau \left\{ D_B \frac{\partial \phi}{\partial y} \frac{\partial T}{\partial y} + \left( \frac{D_T}{D_\infty} \right) \left[ \left( \frac{\partial T}{\partial x} \right)^2 + \left( \frac{\partial T}{\partial y} \right)^2 \right] \right\} \\ & + \frac{v \alpha}{k} \left( \frac{\partial u}{\partial y} \right)^2 + \frac{\alpha \sigma B_0^2 u^2}{k} \end{aligned} \quad (3)$$

(iv) Concentration of nanoparticle:

$$u \frac{\partial \phi}{\partial x} + v \frac{\partial \phi}{\partial y} = D_B \left( \frac{\partial^2 \phi}{\partial x^2} + \frac{\partial^2 \phi}{\partial y^2} \right) + \left( \frac{D_T}{D_\infty} \right) \left[ \left( \frac{\partial T}{\partial x} \right)^2 + \left( \frac{\partial T}{\partial y} \right)^2 \right] \quad (4)$$

(v) Conservation of microorganisms:

$$\begin{aligned} u \frac{\partial n}{\partial x} + v \frac{\partial n}{\partial y} + \frac{b W_c}{(\phi_w - \phi_\infty)} \left[ \frac{\partial}{\partial x} \left( n \frac{\partial \phi}{\partial x} \right) + \frac{\partial}{\partial y} \left( n \frac{\partial \phi}{\partial y} \right) \right] \\ = D_B \left( \frac{\partial^2 n}{\partial x^2} + \frac{\partial^2 n}{\partial y^2} + \frac{\partial^2 n}{\partial x \partial y} \right) \end{aligned} \quad (5)$$

where,  $u$  and  $v$  are the flow constituents along the  $x$  and  $y$  directions correspondingly,  $\rho_f$  is the base liquid density,  $p$  is the liquid pressure,  $T$  is the local temperature,  $\alpha$  is the thermal diffusivity of the base liquid,  $D_B$  is the Brownian diffusion

quantity,  $D_T$  is the thermophoretic diffusion quantity of the,  $D_m$  is the diffusivity of microorganisms,  $g$  is the gravity vector,  $\beta$  is the volume expansion quantity of the liquid,  $\sigma$  is the electrical conductivity of the liquid,  $\mu$  is the viscosity of the liquid,  $\tau = \rho C_p / \rho C_f$  is the ratio of the effective heat capacitance of the nanoparticle to that of the base liquid,  $\gamma$  is the typical volume of a microorganism,  $b$  is the chemotaxis constant,  $W_c$  is maximum cell spinning speed ( $b W_c$  is supposed to be constant),  $n$  is the concentration of the microorganisms,  $\rho_m$  is the microorganisms density,  $\rho_f$  is the base liquid density,  $\phi$  is the nanoparticle capacity fraction.

By using the Rosseland estimate (Brewster [52]), the radiative heat flux in the  $y'$  direction is given by:

$$q_r = -\frac{4\sigma_1}{3k_1} \frac{\partial T^4}{\partial y} \quad (6)$$

where,  $\sigma_1$  is the Stefan-Boltzmann constant and  $k_1$  is the mean absorption quantity.

Presumptuous that the temperature variances within the stream are adequately lesser so that  $T^4$  can be extended in Taylor successions about the free stream temperature  $T_\infty$  to yield:

$$T^4 \cong 4T_\infty^3 T - 3T_\infty^4 \quad (7)$$

where, the higher-order terms of the expansion are ignored. By using (6) and (7), Eq. (3) gives:

$$\begin{aligned} u \frac{\partial T}{\partial x} + v \frac{\partial T}{\partial y} = & \alpha \left( \frac{\partial^2 T}{\partial x^2} + \frac{\partial^2 T}{\partial y^2} \right) - \frac{16\sigma T_\infty^3}{3\rho c_p k_1} \frac{\partial^2 u}{\partial y^2} \\ & + \tau \left\{ D_B \frac{\partial \phi}{\partial y} \frac{\partial T}{\partial y} + \left( \frac{D_T}{D_\infty} \right) \left[ \left( \frac{\partial T}{\partial x} \right)^2 + \left( \frac{\partial T}{\partial y} \right)^2 \right] \right\} \\ & + \frac{v \alpha}{k} \left( \frac{\partial u}{\partial y} \right)^2 + \frac{\alpha \sigma B_0^2 u^2}{k} \end{aligned} \quad (8)$$

We deliberate the borderline conditions,

$$\begin{aligned} u = U_0(x), \quad v = V, \quad T = T_w, \quad \phi = \phi_w, \quad n = n_w \quad \text{at } y = 0 \\ u \rightarrow 0, \quad v \rightarrow 0, \quad T \rightarrow T_\infty, \quad \phi \rightarrow \phi_\infty, \quad n \rightarrow n_\infty \quad \text{as } y \rightarrow \infty \end{aligned} \quad (9)$$

where,  $T_w$ ,  $\phi_w$ ,  $n_w$  are temperature, nanoparticle capacity fraction and density of the motile microorganism at the plate apparent. The corresponding ambient standards are denoted correspondingly by  $T_\infty$ ,  $\phi_\infty$ ,  $n_\infty$ .

Subsequent [25] the free stream flow and the suction/injection flow are expected to be:

$$U_0(x) = ax \quad \text{and} \quad V = -(av)^{1/2} f_w \quad (10)$$

where,  $a > 0$  is the preliminary elongating rate,  $f_w > 0$  signifies transpiration (suction),  $f_w < 0$  resembles to injection and  $f_w = 0$  is the case of an impermeable plate surface.

Presenting the subsequent dimensionless variables and magnitudes:

$$\begin{aligned}
\eta &= y(a/\nu)^{1/2}, \psi = (av)^{1/2} x f(\eta), \\
Gr &= \frac{\beta g \rho_f (1 - \phi_\infty)(T_w - T_\infty)}{a U_0}, \theta(\eta) = \frac{T_f - T_\infty}{T_w - T_\infty}, \\
\xi(\eta) &= \frac{\phi - \phi_\infty}{\phi_w - \phi_\infty}, \chi(\eta) = \frac{n - n_\infty}{n_w - n_\infty}, \\
Nr &= \frac{(\rho_f - \rho_\infty)(\phi_w - \phi_\infty)}{\beta \rho_f (1 - \phi_\infty)(T_w - T_\infty)}, Nb = \frac{\tau D_B (\phi_w - \phi_\infty)}{\alpha}, \\
Nt &= \frac{\tau D_T (\phi_w - \phi_\infty)}{\alpha T_\infty}, Ha = \frac{\sigma B_0^2}{a \rho_f}, \\
\lambda &= ak_0, Pr = \frac{\nu}{\alpha}, Le = \frac{\nu}{D_B}, Lb = \frac{\nu}{D_m}, \\
R &= \frac{4\sigma T_\infty^3}{kk^*}, Ec = \frac{U_0^2}{C_{pf}(T_f - T_\infty)}, \\
Pe &= \frac{bW_c}{D_m}, Rb = \frac{\gamma(n_w - n_\infty)(\rho_m - \rho_f)}{\beta \rho_f (1 - \phi_\infty)(T_w - T_\infty)}, \\
\Omega &= \frac{n_\infty}{(n_w - n_\infty)}
\end{aligned} \tag{11}$$

where,  $\eta$  is the similarity variable and  $\psi$  is the stream purpose defined as:

$$u = \frac{\partial \psi}{\partial y} \text{ and } v = -\frac{\partial \psi}{\partial x} \tag{12}$$

Substituting Eqns. (6) – (9) into Eqns. (1) – (5), we attain the subsequent system of similarity equations:

$$\begin{aligned}
f''' + ff'' - (f')^2 - Haf' \\
-\lambda(f''f'^2 - 2ff'f'') + Gr(\theta - Nr\xi - Rb\chi) = 0
\end{aligned} \tag{13}$$

$$\begin{aligned}
\left(1 + \frac{4}{3}R\right)\theta'' + Pr(f\theta' + Nb\xi') \\
+ Nt(\theta')^2 + Pr Ec(f'')^2 + Ha(f')^2 = 0
\end{aligned} \tag{14}$$

$$\xi'' + Le\xi' + \frac{Nt}{Nb}\theta'' = 0 \tag{15}$$

$$\chi'' + Lb\chi' - Pe[\xi''(\chi + \Omega) + \chi'\xi'] = 0 \tag{16}$$

The boundary conditions becomes:

$$\begin{aligned}
f(0) = f_w, f'(0) = 1, \theta(0) = 1, \\
\xi(0) = 1, \chi(0) = 1, f'(\infty) = 0, \\
\theta(\infty) = 0, \xi(\infty) = 0, \chi(\infty) = 0
\end{aligned} \tag{17}$$

where, primes denote differentiation with respect to  $\eta$ . and  $Ha$  is Hartmann quantity,  $Gr$  is Grashof quantity,  $Nr$  is the buoyancy ratio constraint,  $Rb$  is the bioconvection Rayleigh quantity,  $R$  is the radiation constraint,  $Pr$  is Prandtl quantity,  $Nb$  is the Brownian motion constraint,  $Nt$  is the thermophoresis constraint,  $Ec$  is Eckert quantity,  $Le$  is the traditional Lewis quantity,  $Lb$  is the bioconvection Lewis quantity,  $Pe$  is the bioconvection Peclet quantity,  $\Omega$  is the microorganisms concentration difference constraint and  $f_w$  is the suction/injection constraint.

The quantities of practical interest in this study are the skin

friction  $Cf$ , Nusselt quantity  $Nu$ , Sherwood quantity  $Sh$  and density quantity of the motile microorganisms  $Nn$  defined as:

$$\begin{aligned}
Cf &= \frac{\tau_w}{\rho_f u_0^2}, Nu = \frac{xq_w}{k_f(T_f - T_\infty)}, \\
Sh &= \frac{xq_m}{D_B(\phi_f - \phi_\infty)}, Nn = \frac{xq_n}{k_f(n_f - n_\infty)}
\end{aligned} \tag{18}$$

where,  $\tau_w$ ,  $q_w$ ,  $q_m$  and  $q_n$  are the friction factor, surface heat flux, the surface movement flux and the surface motile microorganisms flux defined by:

$$\begin{aligned}
\tau_w &= \mu \left( \frac{\partial u}{\partial y} \right)_{y=0}, q_w = -k \left. \frac{\partial T}{\partial y} \right|_{y=0}, \\
q_m &= -Db \left. \frac{\partial \xi}{\partial y} \right|_{y=0} \text{ and } q_n = -Dn \left. \frac{\partial \chi}{\partial y} \right|_{y=0}
\end{aligned} \tag{19}$$

Substituting (19) into (18) we obtain,

$$Cf_x = Re_x^{1/2} C_f = f''(0) \tag{20}$$

$$Nu_x = Re_x^{1/2} Nu = -\theta'(0) \tag{21}$$

$$Sh_x = Re_x^{1/2} Sh = -\xi'(0) \tag{22}$$

$$Nn_x = Re_x^{1/2} Nn = -\chi'(0) \tag{23}$$

which are the local friction factor  $Cf_x$ , local Nusselt quantity  $Nu_x$ , local Sherwood quantity  $SH_x$  and local density quantity of the motile microorganisms  $Nn_x$ , correspondingly and  $Re_x = U_\infty x / \nu$  is the Reynolds quantity.

### 3. NUMERICAL PROCEDURE

Under the borderline conditions (17), the set of Eqns. (13)-(16) are combined nonlinear boundary value problems (BVPs) that are numerically solved using a shooting approach with a Runge–Kutta Fehlberg integration pattern. The fourth order Runge–Kutta Fehlberg iteration pattern is used to integrate the collection of IVPs until the stated boundary conditions are met, after which the equation is converted into a set of initial value problems (IVP) with unknown initial values that must be established by guessing.

New variables are created:

$$\begin{aligned}
x_1 = f, x_2 = f', x_3 = f'', \\
x_4 = \theta, x_5 = \theta', x_6 = \xi, \\
x_7 = \xi', x_8 = \chi, x_9 = \chi'
\end{aligned} \tag{24}$$

Eqns. (13) and (16) are then condensed to systems of first order differential equations as:

$$x_3' = -x_1 x_3 + x_2^2 + Hax_2 - Gr(x_4 - Nrx_6 - Rbx_8) \tag{25}$$

$$\begin{aligned}
x_5' &= -\frac{1}{(1 + 4R/3)} x_5 (Pr x_1 - Nbx_7) \\
&- Nt x_5^2 - Pr Ec(x_3^2 + Hax_2^2)
\end{aligned} \tag{26}$$

$$x_7' = -Lex_1x_7 - \frac{Nt}{Nb} \left[ -x_5(\text{Pr}x_1 - Nbx_7) - Ntx_5^2 - \text{Pr}Ec(x_3^2 + Hax_2^2) \right] \quad (27)$$

$$x_9' = -Lbx_1x_9 - Pe \left\{ (x_8 + \Omega) \left[ -Lex_1x_7 - \frac{Nt}{Nb} \left[ -x_5(\text{Pr}x_1 - Nbx_7) - Ntx_5^2 - \text{Pr}Ec(x_3^2 + Hax_2^2) + x_7x_9 \right] \right] \right\} \quad (28)$$

subject to the following initial conditions.

$$\begin{aligned} x_1(0) = fw, \quad x_2(0) = 1, \quad x_3(0) = s_1, \quad x_4(0) = 1, \\ x_5(0) = s_2, \quad x_6(0) = s_3, \quad x_7(0) = s_3, \quad x_8(0) = s_4, \quad x_9(0) = s_4 \end{aligned} \quad (29)$$

In the shooting technique, the unknown initial conditions  $s_1, s_2, s_3$  and  $s_4$  in (29) are supposed and (25)-(28) integrated numerically as an initial value problem to a given terminal point. The accuracy of the assumed missing initial conditions was checked by comparing the calculated value of the dependent variable at the terminal point with its given value there. If variances exist, better values of the missing initial conditions are attained and the procedure repetitive. From the practice of numerical computation, the liquid flow, the temperature, the friction factor  $t$ , the Nusselt quantity, the local Sherwood quantity and local density quantity of the motile microorganisms are comparative to  $f(\eta), g(\eta), f(0), \theta(0), C(0)$  and  $\chi(0)$ , respectively.

#### 4. RESULTS AND DISCUSSION

For designs of the results, numerical values are connived in Figures 1-26 and a comprehensive debate on the possessions of the leading constraints, specifically bioconvection Lewis quantity  $Lb$ , traditional Lewis quantity  $Le$ , bioconvection Péclet quantity  $Pe$ , buoyancy ratio constraint  $Nr$ , bioconvection Rayleigh quantity  $Rb$ , Brownian motion constraint  $Nb$ , thermophoresis constraint  $Nt$ , Hartmann quantity  $Ha$ , Grashof quantity  $Gr$ , Eckert quantity  $Ec$ , the microorganisms concentration difference constraint  $\Omega$  and the suction/injection constraint  $fw$  on the flow, temperature, nanoparticles volume fraction and motile microorganisms density outlines as well as the friction factor, the local Nusselt quantity, the local Sherwood quantity, the local density quantity of the motile microorganisms is carried out in this section for constant value of  $\text{Pr}=0.71$ .

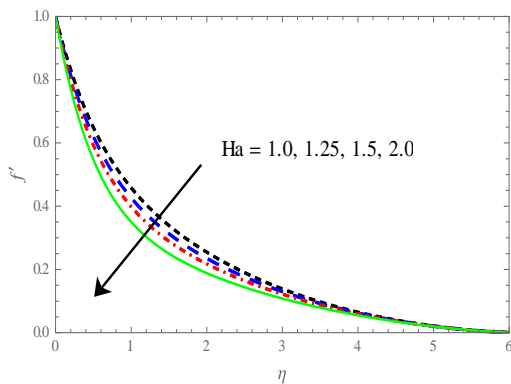


Figure 1. Influence of  $Ha$  on  $f'(n)$

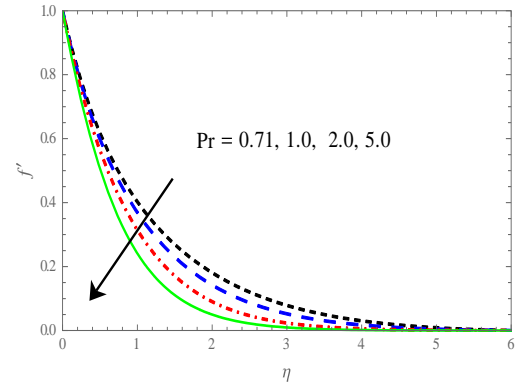


Figure 2. Influence of  $Pr$  on  $f'(n)$

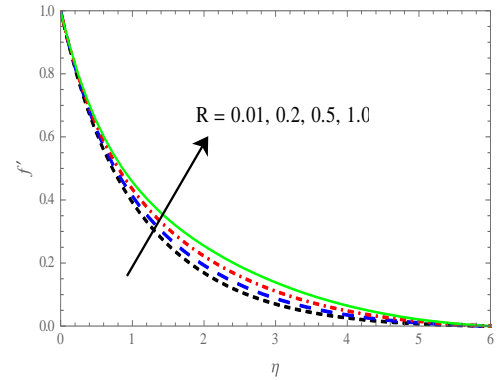


Figure 3. Influence of  $R$  on  $f'(n)$

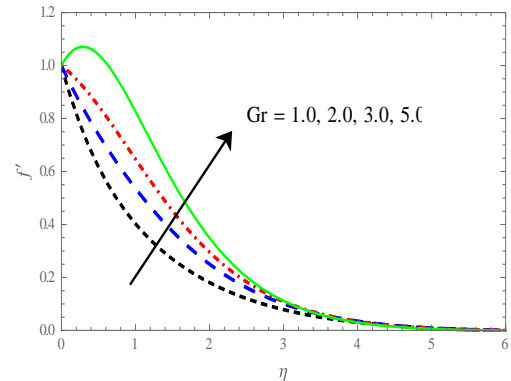


Figure 4. Influence of  $Gr$  on  $f'(n)$

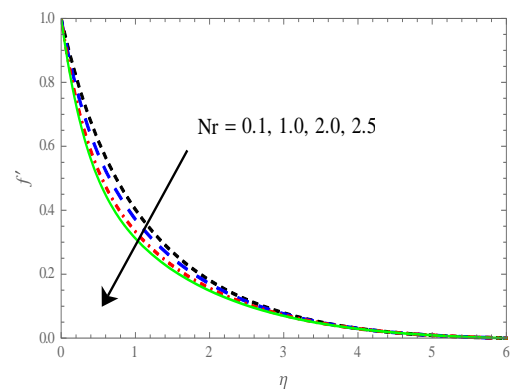
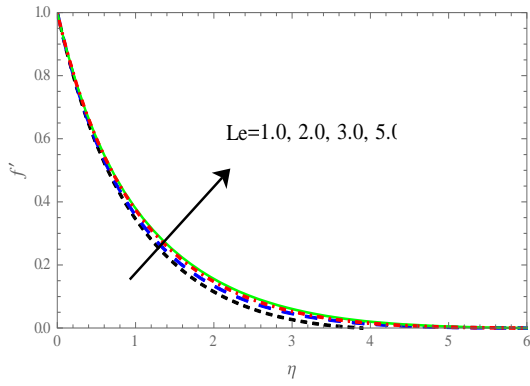
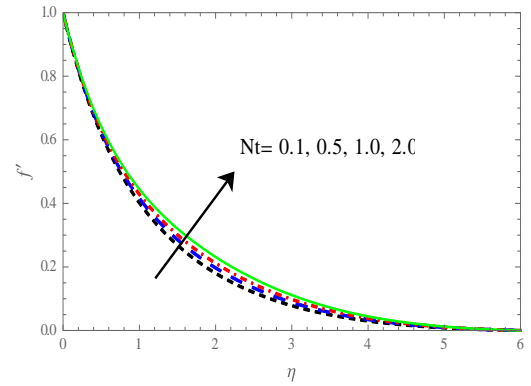


Figure 5. Influence of  $Nr$  on  $f'(n)$



**Figure 6.** Influence of  $Le$  on  $f'(n)$



**Figure 10.** Influence of  $Nt$  on  $f'(n)$

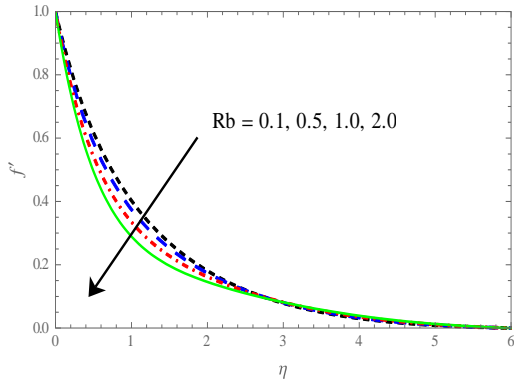


**Figure 7.** Influence of  $Rb$  on  $f'(n)$

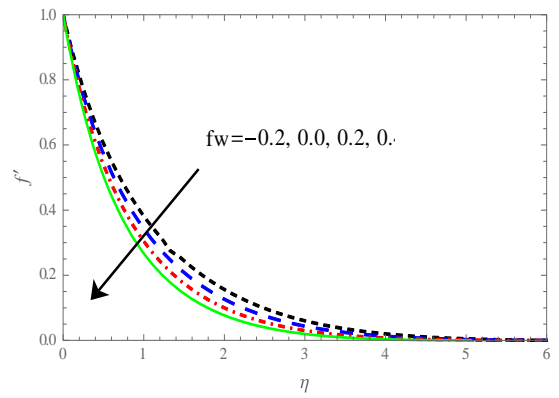


**Figure 11.** Influence of  $fw$  on  $f'(n)$

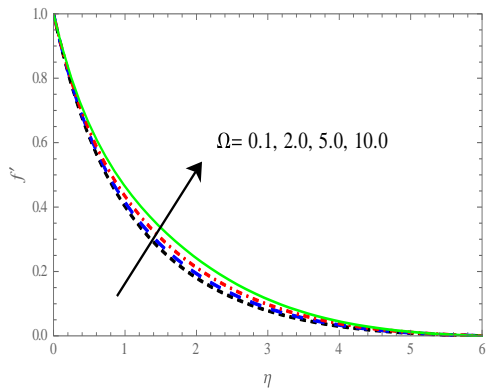


**Figure 8.** Influence of  $\Omega$  on  $f'(n)$

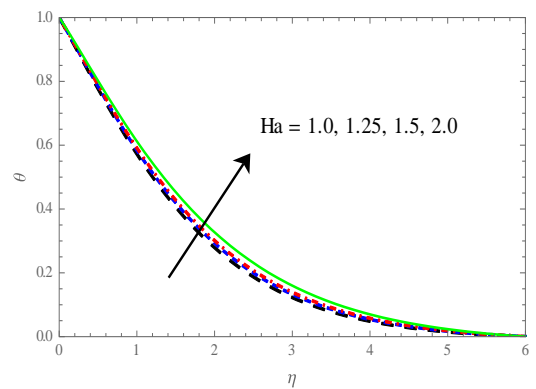


**Figure 12.** Influence of  $Ha$  on  $\theta(n)$

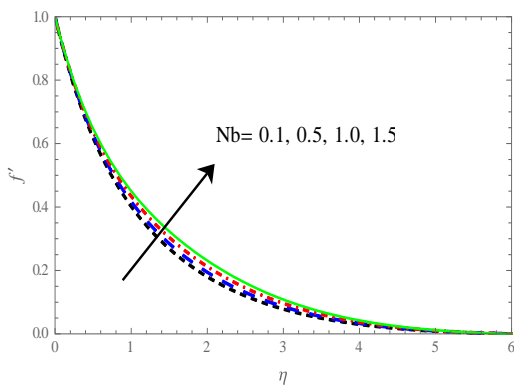


**Figure 9.** Influence of  $Nb$  on  $f'(n)$

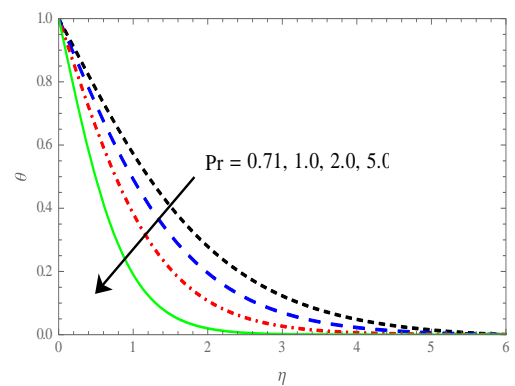


**Figure 13.** Influence of  $Pr$  on  $\theta(n)$

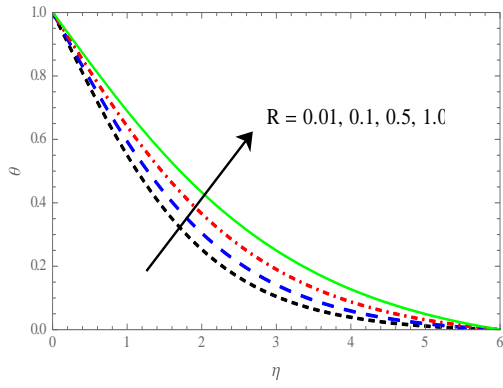


**Figure 14.** Influence of  $R$  on  $\theta(n)$

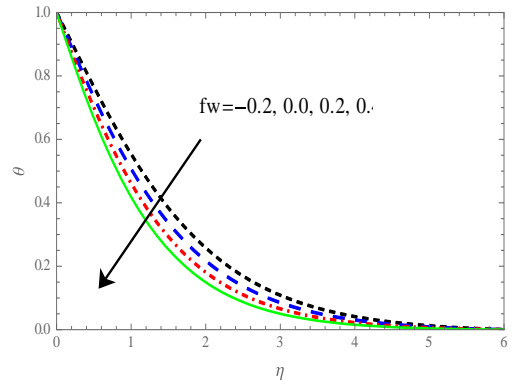


**Figure 18.** Influence of  $fw$  on  $\theta(n)$

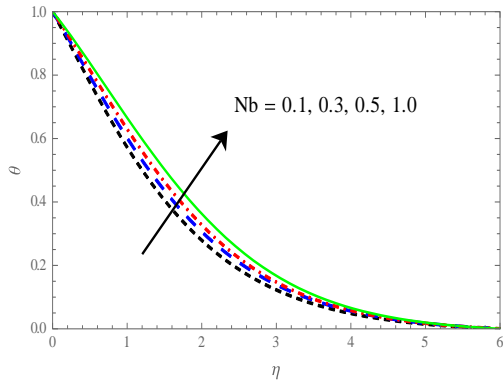


**Figure 15.** Influence of  $Nb$  on  $\theta(n)$

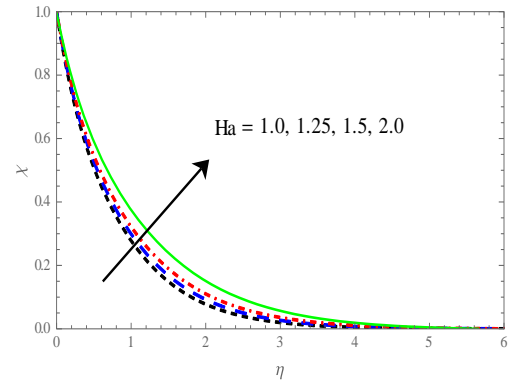


**Figure 19.** Influence of  $Ha$  on  $\chi(n)$

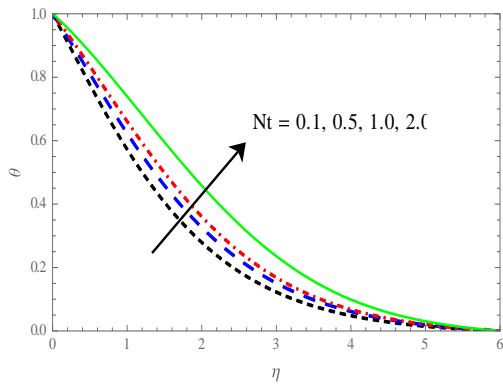


**Figure 16.** Influence of  $Nt$  on  $\theta(n)$

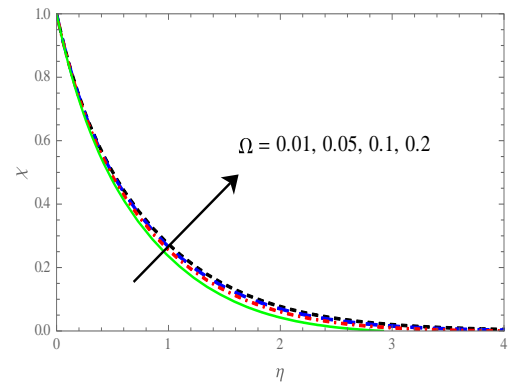


**Figure 20.** Influence of  $\Omega$  on  $\chi(n)$

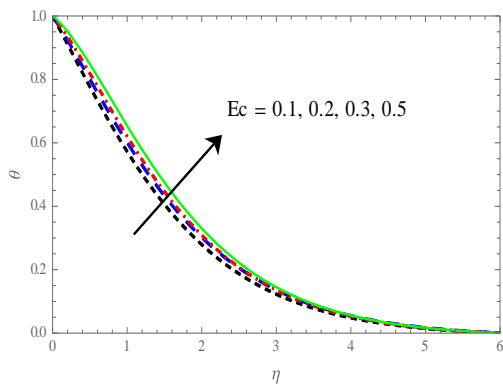


**Figure 17.** Influence of  $Ec$  on  $\theta(n)$

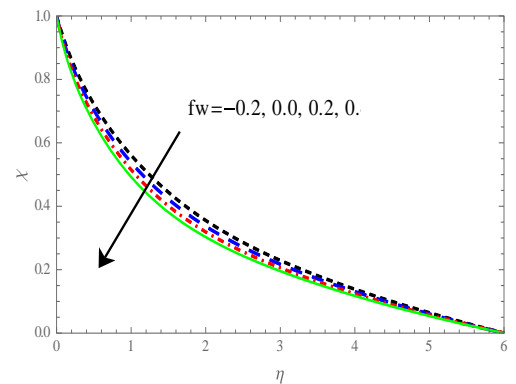


**Figure 21.** Influence of  $fw$  on  $\chi(n)$

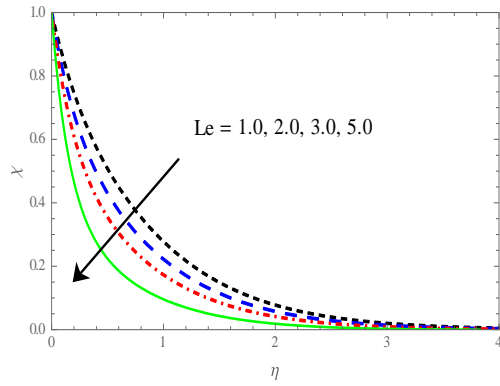


**Figure 22.** Influence of  $Le$  on  $\chi(n)$

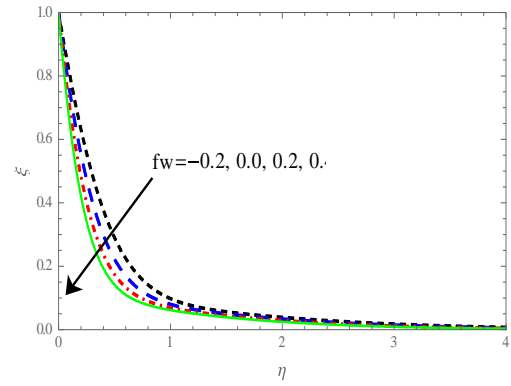


**Figure 26.** Influence of  $fw$  on  $\chi(n)$

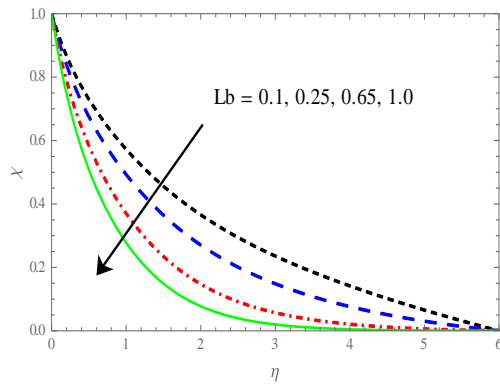


**Figure 23.** Influence of  $Lb$  on  $\chi(n)$

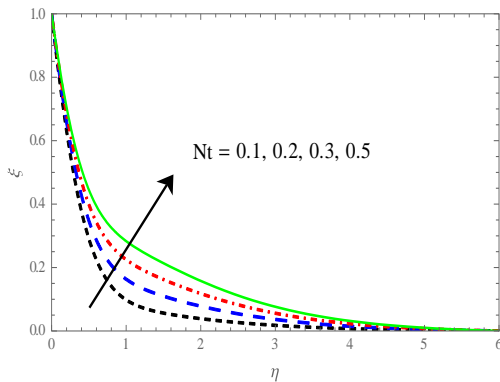


**Figure 24.** Influence of  $Nt$  on  $\zeta(n)$

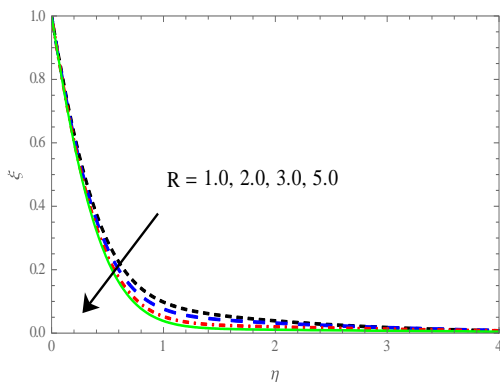


**Figure 25.** Influence of  $R$  on  $\zeta(n)$

#### 4.1 Flow outlines

Figures 1-11, correspondingly demonstration the effect of the several values of the constraints  $Ha$ ,  $Pr$ ,  $R$ ,  $Nt$ ,  $Nb$ ,  $Gr$ ,  $R$ ,  $Nr$ ,  $Le$ ,  $Rb$ ,  $\Omega$  and  $fw$  on the flow outlines. In Figure 1, we perceive that due to rise in Hartmann quantity  $Ha$ , there is a drop in the flow supply. In accumulation, we find that the flow declines as Prandtl quantity  $Pr$  escalations, as plotted in Figure 2. Figure 3 confirmations that the flow profile upsurges when radiation constraints  $R$  rise. We perceive from Figure 4 that as Grashof quantity  $Gr$  elevations the flow profile rises. Figure 5 portrays that the flow declines as buoyancy ratio constraint  $Nr$  escalations. We also perceive from Figure 6 that as the traditional Lewis quantity  $Le$  growths the flow profile intensifications. The influence of bioconvection Rayleigh quantity  $Rb$  on flow outlines is exposed in Figure 7. It is initiate that flow declines with growing values of  $Rb$ . Further, it is clear from Figure 8-10 that as the Brownian motion constraint  $Nb$  and thermophoresis constraint  $Nt$  and microorganisms concentration change constraint  $\Omega$  upsurges, the flow profile increases, but it declines when the suction constraint  $fw$  rises as shown in Figure 11.

#### 4.2 Temperature outlines

The variations of temperature outlines for dissimilar values of the constraints  $Ha$ ,  $Pr$ ,  $R$ ,  $Nt$ ,  $Nb$ ,  $Ec$  and  $fw$  in the figures 12–18 are revealed. Figure 12 elucidates that as Hartmann quantity  $Ha$  surges the temperature rises. In addition, the temperature outlines decline as Prandtl quantity  $Pr$  rises as shown in Figure 13. In Figure 14, we notice that due to an intensification in radiation constraint  $R$ , there is a rise in the temperature outline. From Figure 15-17, we may observe that the temperature outline rises as the Brownian motion constraint  $Nb$  and thermophoresis constraint  $Nt$  and Eckert quantity  $Ec$  upsurges, while Figure 18 shows that it declines when the suction constraint  $fw$  rises.

#### 4.3 Nanoparticle concentration outlines

Figures 19-23 signify the nanoparticle concentration outlines with dissimilar constraints  $Ha$ ,  $\Omega$ ,  $Le$ ,  $Lb$  and  $fw$ . Figure 19 shows that as Hartmann quantity  $Ha$  rises the nanoparticle concentration outlines upsurges. In addition, the nanoparticle concentration outlines surges as microorganisms concentration difference constraint  $\Omega$  rises as shown in Figure 20. In Figure 21, we notice that due to rise in the traditional Lewis quantity  $Le$ , there is decline in nanoparticle concentration outlines. From Figure 22, we may observe that

the nanoparticle concentration outlines decline as the bioconvection Lewis quantity  $Lb$ , while Figure 23 demonstrates that it declines when the suction constraint  $fw$  rises.

#### 4.4 Motile microorganisms density outlines

The effects of the numerous pertinent constraints  $Nt$ ,  $R$  and  $fw$  on the dimensionless density of motile microorganisms are scrutinised in Figure 24–26. The dimensionless density of motile microorganisms rises as buoyancy ratio constraint  $Nr$  surges is shown in Figure 24. In Figure 25, we perceive that due to rise in the radiation constraint  $R$ , there is decline in the dimensionless density of motile microorganisms' outlines. On

the other hand, the dimensionless density of motile microorganisms declines with a rise suction constraint  $fw$  as shown in Figure 26.

#### 4.5 Effects of constraint variations on $Nu_x$ , $Sh_x$ , $Nn_x$

Table 1 shows that Demonstrates the effects of many thermophysical constraints  $Nt$ ,  $Nb$ ,  $Pe$ ,  $R$ ,  $Ec$ ,  $Rb$  and  $Le$  on the local Nusselt quantity, the local Sherwood quantity and the density quantity motile microorganisms. It is apparent that all constraints accumulative effects on local Sherwood quantity  $Sh_x$ . In addition, the rate of heat transport portrayed by the local Nusselt quantity and the density quantity motile microorganisms on wall upsurge with cumulative values of  $Pe$  and  $Le$ , but they decline with climb of  $Nt$ ,  $Nb$ ,  $R$ ,  $Ec$  and  $Rb$ .

**Table 1.** Numerical values of the local Sherwood quantity and wall motile microorganisms flux corresponding to dissimilar values  $Nb$  and  $Nt$

$Nt$	$Nb$	$Pe$	$R$	$Ec$	$Rb$	$Le$	$Nu_x$	$Sh_x$	$Dm_x$
0.10	0.10	1.0	0.01	0.01	0.10	0.10	0.460041	2.08574	0.817714
0.15							0.428209	2.11859	0.813935
0.20							0.418146	2.15398	0.792693
0.10	0.1						0.460041	2.08574	0.817714
	0.2						0.438792	2.22898	0.796824
	0.3						0.418576	2.25005	0.712850
	0.1	1.0					0.460041	2.08574	0.817714
		2.0					0.462855	2.08828	1.962055
		3.0					0.464834	2.09031	3.694051
		1.0	0.01				0.460041	2.08574	0.817714
			0.05				0.448461	2.09496	0.808462
			0.1				0.435158	2.10513	0.797722
			0.01	0.01			0.511274	2.04269	0.873675
				0.05			0.488501	2.06184	0.849025
				0.10			0.460041	2.08574	0.817714
				0.01	0.1		0.460041	2.08574	0.817714
					0.2		0.438792	2.19283	0.813935
					0.3		0.418576	2.22898	0.796824
					0.1	0.1	0.460041	2.08574	0.817714
						0.2	0.460796	2.08631	0.903403
						0.3	0.461435	2.08682	0.990881

## 5. CONCLUSIONS

The boundary layer stream of a water-based nanoliquid comprising motile microorganisms past a vertical permeable flat plate is considered numerically. The convective procedure is controlled by the buoyancy constraint  $Nr$  and bioconvection constraints  $Pe$ ,  $Lb$  and  $Rb$ . Based on the numerical results, the following summary is arrived at.

(1) Both the liquid flow declines and the hydrodynamic border layer thickness declines with intensification in  $Rb$ ,  $Nr$ ,  $Ha$ ,  $fw$ , while the converse is true for amplified  $Nt$ ,  $Nb$ ,  $Gr$ ,  $Ec$ ,  $\Omega$  and  $fw$ .

(2) Cumulative the  $Ec$ ,  $Nt$ ,  $Nb$ ,  $Ha$  and  $fw$ , lead to an escalation in both the liquid temperature and the thermal boundary layer thickness with a converse effect noted with escalation in  $fw$ .

(3) An escalation in  $Rb$ ,  $Ha$ ,  $Nt$ ,  $Nr$  intensifications the dimensionless nanoparticle concentration, whereas, the reverse is pragmatic with improved  $Le$ ,  $fw$ ,  $Gr$ ,  $Nb$  and  $Ec$ .

(4) Growing  $Lb$ ,  $fw$ ,  $Pe$  and  $\Omega$  diminishes the dimensionless microorganism conservation, while an escalation is pragmatic on the same with improved  $Nr$ ,  $Rb$  and  $Ha$ .

(5) An escalation in  $Nt$ ,  $Nb$ ,  $Pe$ ,  $R$ ,  $Ec$ ,  $Rb$  and  $Le$  leads to an escalation in the local Sherwood quantity.

(6) Accumulative  $Pe$  and  $Le$  upsurges both the Nusselt quantity and the local density quantity of the motile microorganisms but they reduction with cumulative  $Nt$ ,  $Nb$ ,  $Pe$ ,  $R$ ,  $Ec$  and  $Rb$ .

## REFERENCES

- [1] Kuznetsov, A.V. (2011). Bio-thermal convection induced by two different species of microorganisms. *International Communications in Heat and Mass Transfer*, 38(5): 548-553. <https://doi.org/10.1016/j.icheatmasstransfer.2011.02.006>
- [2] Kuznetsov, A.V. (2006). The onset of thermo-bioconvection in a shallow fluid saturated porous layer heated from below in a suspension of oxytactic microorganisms. *European Journal of Mechanics-B/Fluids*, 25(2): 223-233. <https://doi.org/10.1016/j.euromechflu.2005.06.003>
- [3] Hill, N.A., Pedley, T.J. (2005). Bioconvection. *Fluid Dynamics Research*, 37(1-2): 1. <https://doi.org/10.1016/j.fluiddyn.2005.03.002>
- [4] Nield, D.A., Kuznetsov, A.V. (2006). The onset of bio-

- thermal convection in a suspension of gyrotactic microorganisms in a fluid layer: Oscillatory convection. *International Journal of Thermal Sciences*, 45(10): 990-997. <https://doi.org/10.1016/j.ijthermalsci.2006.01.007>
- [5] Avramenko, A.A., Kuznetsov, A.V. (2004). Stability of a suspension of gyrotactic microorganisms in superimposed fluid and porous layers. *International Communications in Heat and Mass Transfer*, 31(8): 1057-1066. <https://doi.org/10.1016/j.icheatmasstransfer.2004.08.003>
- [6] Alloui, Z., Nguyen, T.H., Bilgen, E. (2007). Numerical investigation of thermo-bioconvection in a suspension of gravitactic microorganisms. *International Journal of Heat and Mass Transfer*, 50(7-8): 1435-1441. <https://doi.org/10.1016/j.ijheatmasstransfer.2006.09.008>
- [7] Spormann, A.M. (1987). Unusual swimming behavior of a magnetotactic bacterium. *FEMS Microbiology Ecology*, 3(1): 37-45.
- [8] Pedley, T.J., Hill, N.A., Kessler, J.O. (1988). The growth of bioconvection patterns in a uniform suspension of gyrotactic micro-organisms. *Journal of Fluid Mechanics*, 195: 223-237. <https://doi.org/10.1017/S0022112088002393>
- [9] Hill, N.A., Pedley, T.J., Kessler, J.O. (1989). Growth of bioconvection patterns in a suspension of gyrotactic micro-organisms in a layer of finite depth. *Journal of Fluid Mechanics*, 208: 509-543. <https://doi.org/10.1017/S0022112089002922>
- [10] Sokolov, A., Goldstein, R.E., Feldchtein, F.I., Aranson, I.S. (2009). Enhanced mixing and spatial instability in concentrated bacterial suspensions. *Physical Review E*, 80(3): 031903. <https://doi.org/10.1103/PhysRevE.80.031903>
- [11] Tsai, T.H., Liou, D.S., Kuo, L.S., Chen, P.H. (2009). Rapid mixing between ferro-nanofluid and water in a semi-active Y-type micromixer. *Sensors and Actuators A: Physical*, 153(2): 267-273. <https://doi.org/10.1016/j.sna.2009.05.004>
- [12] Kuznetsov, A.V. (2010). The onset of nanofluid bioconvection in a suspension containing both nanoparticles and gyrotactic microorganisms. *International Communications in Heat and Mass Transfer*, 37(10): 1421-1425. <https://doi.org/10.1016/j.icheatmasstransfer.2010.08.015>
- [13] Kuznetsov, A.V. (2011). Nanofluid bioconvection in water-based suspensions containing nanoparticles and oxytactic microorganisms: Oscillatory instability. *Nanoscale Research Letters*, 6(1): 1-13. <https://doi.org/10.1186/1556-276X-6-100>
- [14] Kuznetsov, A.V. (2011). Non-oscillatory and oscillatory nanofluid bio-thermal convection in a horizontal layer of finite depth. *European Journal of Mechanics-B/Fluids*, 30(2): 156-165. <https://doi.org/10.1016/j.euromechflu.2010.10.007>
- [15] Buongiorno, J. (2006). Convective transport in nanoliquids. *Journal of Heat Transport*, 128(3): 240-250. <https://doi.org/10.1115/1.2150834>
- [16] Kakaç, S., Pramuanjaroenkij, A. (2009). Review of convective heat transfer enhancement with nanofluids. *International Journal of Heat and Mass Transfer*, 52(13-14): 3187-3196. <https://doi.org/10.1016/j.ijheatmasstransfer.2009.02.006>
- [17] Lee, J.H., Lee, S.H., Choi, C., Jang, S., Choi, S. (2011). A review of thermal conductivity data, mechanisms and models for nanofluids. *International Journal of Micro-Nano Scale Transport*, 1(4): 269-322. <http://dx.doi.org/10.1260/1759-3093.1.4.269>
- [18] Wong, K.V., De Leon, O. (2017). Applications of nanofluids: current and future. In *Nanotechnology and Energy*, pp. 105-132.
- [19] Siddiq, S., Begum, N., Saleem, S., Hossain, M.A., Gorla, R.S.R. (2016). Numerical solutions of nanofluid bioconvection due to gyrotactic microorganisms along a vertical wavy cone. *International Journal of Heat and Mass Transfer*, 101: 608-613. <https://doi.org/10.1016/j.ijheatmasstransfer.2016.05.076>
- [20] Aziz, A., Khan, W.A., Pop, I. (2012). Free convection boundary layer flow past a horizontal flat plate embedded in porous medium filled by nanofluid containing gyrotactic microorganisms. *International Journal of Thermal Sciences*, 56: 48-57. <https://doi.org/10.1016/j.ijthermalsci.2012.01.011>
- [21] Wang, S., Tan, W. (2011). Stability analysis of solet-driven double-diffusive convection of Maxwell fluid in a porous medium. *International Journal of Heat and Fluid Flow*, 32(1): 88-94. <https://doi.org/10.1016/j.ijheatfluidflow.2010.10.005>
- [22] Nadeem, S., Haq, R.U., Khan, Z.H. (2014). Numerical study of MHD boundary layer flow of a Maxwell fluid past a stretching sheet in the presence of nanoparticles. *Journal of the Taiwan Institute of Chemical Engineers*, 45(1): 121-126. <https://doi.org/10.1016/j.jtice.2013.04.006>
- [23] Ramzan, M., Bilal, M., Chung, D.J., Farooq, U. (2016). Sundry convective stream of Maxwell nanoliquid past a porous vertical stretched surface-An optimal solution. *Results in Physics*, 6: 1072-1079.
- [24] Nagendramma, V., Kumar, R.K., Prasad, P.D., Leelaratham, A., Varma, S.V.K. (2016). Multiple slips and radiation effects on Maxwell nanofluid flow over a permeable stretching surface with dissipation. *Journal of Nanofluids*, 5(6): 817-825. <https://doi.org/10.1166/jon.2016.1273>
- [25] Hayat, T., Muhammad, T., Shehzad, S.A., Alsaedi, A. (2015). Three dimensional boundary layer stream of Maxwell nanoliquid: Mathematical model. *Applied Mathematics and Mechanics-English Edition*, 36(3): 747-762.
- [26] Sadeghy, K., Najafi, A.H., Saffaripour, M. (2005). Sakiadis flow of an upper-convected Maxwell fluid. *International Journal of Non-Linear Mechanics*, 40(9): 1220-1228. <https://doi.org/10.1016/j.ijnonlinmec.2005.05.006>
- [27] Motsa, S.S., Hayat, T., Aldossary, O.M. (2012). MHD flow of upper-convected Maxwell fluid over porous stretching sheet using successive Taylor series linearization method. *Applied Mathematics and Mechanics*, 33(8): 975-990. <https://doi.org/10.1007/s10483-012-1599-x>
- [28] Hayat, T., Iqbal, Z., Mustafa, M., Alsaedi, A. (2012). Momentum and heat transport of an upper convected Maxwell liquid over a moving surface with convective boundary conditions. *Nuclear Eng Des.*, 252(2012): 242-247.
- [29] Vajravelu, K., Prasad, K.V., Santhi, S.R. (2015). Heat transfer in an upper convected maxwell fluid with fluid

- particle suspension. *Advances in Applied Mathematics and Mechanics*, 7(3): 369-386. <https://doi.org/10.4208/aamm.2013.m379>
- [30] Kuznetsov, A.V. (2005). Thermo-bioconvection in a suspension of oxytactic bacteria. *International Communications in Heat and Mass Transfer*, 32(8): 991-999. <https://doi.org/10.1016/j.icheatmasstransfer.2004.11.005>
- [31] Kuznetsov, A.V. (2005). The onset of bioconvection in a suspension of gyrotactic microorganisms in a fluid layer of finite depth heated from below. *International Communications in Heat and Mass Transfer*, 32(5): 574-582. <https://doi.org/10.1016/j.icheatmasstransfer.2004.10.021>
- [32] Kuznetsov, A.V. (2005). Investigation of the onset of thermo-bioconvection in a suspension of oxytactic microorganisms in a shallow fluid layer heated from below. *Theoretical and Computational Fluid Dynamics*, 19(4): 287-299. <https://doi.org/10.1007/s00162-005-0167-3>
- [33] Geng, P., Kuznetsov, A.V. (2004). Effect of small solid particles on the development of bioconvection plumes. *International Communications in Heat and Mass Transfer*, 31(5): 629-638. [https://doi.org/10.1016/S0735-1933\(04\)00050-8](https://doi.org/10.1016/S0735-1933(04)00050-8)
- [34] Geng, P., Kuznetsov, A.V. (2005). Settling of bidispersed small solid particles in a dilute suspension containing gyrotactic micro-organisms. *International Journal of Engineering Science*, 43(11-12): 992-1010. <https://doi.org/10.1016/j.ijengsci.2005.03.002>
- [35] Geng, P., Kuznetsov, A.V. (2005). Introducing the concept of effective diffusivity to evaluate the effect of bioconvection on small solid particles. *International Journal of Transport Phenomena*, 7(4): 321-338.
- [36] Zaimi, K., Ishak, A., Pop, I. (2014). Stagnation-point stream toward stretching/shrinking sheet in a nanoliquid containing both nanoparticles and gyrotactic microorganisms. *J Heat Transf.*, 136: 041705.
- [37] Tham, L., Nazar, R., Pop, I. (2013). Sundry convection stream over a solid sphere embedded in a porous medium filled by a nanoliquid containing gyrotactic microorganisms. *Int J Heat Movementum Transf.*, 62: 647-660.
- [38] Xu, H., Pop, I. (2014). Fully developed sundry convection stream in a horizontal channel filled by a nanoliquid containing both nanoparticles and gyrotactic microorganisms. *Euro J Mech B/Liquids.*, 46: 37-45.
- [39] Khan, W.A., Uddin, M., Ismail, A.I. (2013). Free convection of non-Newtonian nanofluids in porous media with gyrotactic microorganisms. *Transport in Porous Media*, 97(2): 241-252. <https://doi.org/10.1007/s11242-012-0120-z>
- [40] Ibrahim, W., Makinde, O.D. (2013). The effect of double stratification on boundary-layer flow and heat transfer of nanofluid over a vertical plate. *Computers & Fluids*, 86: 433-441. <https://doi.org/10.1016/j.compfluid.2013.07.029>
- [41] Alsaedi, A., Khan, M.I., Farooq, M., Gull, N., Hayat, T. (2017). Magnetohydrodynamic (MHD) stratified bioconvective flow of nanofluid due to gyrotactic microorganisms. *Advanced Powder Technology*, 28(1): 288-298. <https://doi.org/10.1016/j.appt.2016.10.002>
- [42] Ramzan, M., Chung, J.D., Ullah, N. (2017). Radiative magnetohydrodynamic nanofluid flow due to gyrotactic microorganisms with chemical reaction and non-linear thermal radiation. *International Journal of Mechanical Sciences*, 130: 31-40. <https://doi.org/10.1016/j.ijmecsci.2017.06.009>
- [43] Srinivasacharya, D., Surender, O. (2015). Effect of double stratification on sundry convection boundary layer stream of a nanoliquid past a vertical plate in a porous medium. *Applied Nanoscience*, 5: 29-38.
- [44] Hayat, T., Hussain, T., Shehzad, S.A., Alsaedi, A. (2014). Thermal and concentration stratifications effects in radiative flow of Jeffrey fluid over a stretching sheet. *Plos One*, 9(10): e107858. <https://doi.org/10.1371/journal.pone.0107858>
- [45] Hayat, T., Qayyum, S., Farooq, M., Alsaedi, A., Ayub, M. (2015). Sundry convection stream of Jeffrey liquid along an inclined elongating cylinder with double stratification effect. *Thermal Science*.
- [46] Hayat, T., Imtiaz, M., Alsaedi, A. (2016). Unsteady stream of nanoliquid with double stratification and magnetohydrodynamics. *Int J Heat Movementum Transf.*, 92: 100-109.
- [47] Jamil, M., Fetecau, C. (2010). Helical streams of maxwell liquid between coaxial cylinders with given shear stresses on the boundary. *Nonlinear Analysis: Real World Applications*, 5: 4302-4311.
- [48] Zierep, J., Fetecau, C. (2007). Energetic balance for the Rayleigh–Stokes problem of a Maxwell fluid. *International Journal of Engineering Science*, 45(2-8): 617-627. <https://doi.org/10.1016/j.ijengsci.2007.04.015>
- [49] Hayat, T., Waqas, M., Shehzad, S.A., Alsaedi A. (2014). Effects of joule heating and thermophoresis on stretched stream with convective boundary conditions. *Sci Iran.*, 21(3): 682-692.
- [50] Hsiao, K.L. (2017). Combined electrical MHD heat transfer thermal extrusion system using Maxwell fluid with radiative and viscous dissipation effects. *Applied Thermal Engineering*, 112: 1281-1288. <https://doi.org/10.1016/j.applthermaleng.2016.08.208>
- [51] Ramzan, M., Bilal, M., Chung, J.D. (2017). Influence of homogeneous-heterogeneous reactions on MHD 3D Maxwell fluid flow with Cattaneo-Christov heat flux and convective boundary condition. *Journal of Molecular Liquids*, 230: 415-422. <https://doi.org/10.1016/j.molliq.2017.01.061>
- [52] Brewster, M.Q. (1992). *Thermal Radiative Transport and Properties*. John Wiley and Sons, New York.